



Published in final edited form as:

Dev Cell. 2014 September 29; 30(6): 759–767. doi:10.1016/j.devcel.2014.07.016.

Four GTPases Differentially Regulate the Sec7 Arf-GEF to Direct Traffic at the *trans*-Golgi Network

Caitlin M. McDonold¹ and J. Christopher Fromme^{1,*}

¹Department of Molecular Biology and Genetics, Weill Institute for Cell and Molecular Biology, Cornell University, Ithaca, NY, 14853, USA

Abstract

Summary—Traffic through the Golgi complex is controlled by small GTPases of the Arf and Rab families. Guanine nucleotide exchange factor (GEF) proteins activate these GTPases to control Golgi function, yet the full assortment of signals regulating these GEFs is unknown. The Golgi Arf-GEF Sec7 and the homologous BIG1/2 proteins are effectors of the Arf1 and Arl1 GTPases. We demonstrate that Sec7 is also an effector of two Rab GTPases, Ypt1 (Rab1) and Ypt31/32 (Rab11), signifying unprecedented signaling cross-talk between GTPase pathways. The molecular basis for the role of Ypt31/32 and Rab11 in vesicle formation has remained elusive. We find that Arf1, Arl1, and Ypt1 primarily affect the membrane localization of Sec7, whereas Ypt31/32 exerts a dramatic stimulatory effect on the nucleotide exchange activity of Sec7. The convergence of multiple signaling pathways on a master regulator reveals a mechanism for balancing incoming and outgoing traffic at the Golgi.

Introduction

The Golgi complex is the primary sorting organelle of the eukaryotic secretory pathway. Traffic through the Golgi depends on the action of small GTPases of the Arf and Rab families (Barr, 2009; Donaldson and Jackson, 2011). Arf proteins primarily regulate outgoing vesicle biogenesis pathways by recruiting vesicle coat proteins and lipid-modifying enzymes. Rab proteins primarily regulate the transport, tethering, and fusion of incoming vesicles. Notable exceptions include Rab6 and the Rab11 homologs Ypt31/32, which also appear to play direct roles in vesicle biogenesis (Benli et al., 1996; Jedd et al., 1997; Miserey-Lenkei et al., 2010), although the role of Ypt31/32 in vesicle biogenesis is unknown. GEFs activate Arf and Rab proteins to govern incoming and outgoing traffic at the Golgi (Mizuno-Yamasaki et al., 2012), but it is unknown how these GEFs are regulated by organelle status and cargo flux. In particular, there is scant evidence of significant coordination between Arf and Rab pathways at the Golgi.

© 2014 Elsevier Inc. All rights reserved

*Correspondence: jcf14@cornell.edu.

Publisher's Disclaimer: This is a PDF file of an unedited manuscript that has been accepted for publication. As a service to our customers we are providing this early version of the manuscript. The manuscript will undergo copyediting, typesetting, and review of the resulting proof before it is published in its final citable form. Please note that during the production process errors may be discovered which could affect the content, and all legal disclaimers that apply to the journal pertain.

Multiple Arf-dependent vesicle pathways sort cargos from the trans-Golgi network (TGN) to endosomes, the lysosome, and the plasma membrane (PM). Cargo sorting at the TGN depends upon Arf activation by the Arf-GEF Sec7 in yeast and its homologs BIG1/2 in mammalian cells (Casanova, 2007). Sec7 is regulated through positive feedback by Arf1 (Richardson et al., 2012), and BIG1/2 is regulated by both Arf and Arl1 GTPases (Christis and Munro, 2012; Lowery et al., 2013).

Here we report that in addition to being an effector of Arf1 and Arl1, Sec7 is also an effector of two Rab proteins, Ypt1 (Rab1) and Ypt31/32 (Rab11). Therefore, four distinct GTPases directly regulate Sec7. We show that Ypt1 primarily affects the localization of Sec7 and exerts a modest effect on Sec7 activity. In contrast, Ypt31/32 exerts a dramatic stimulatory effect on the activity of Sec7. We find that TGN cargo sorting in yeast appears to occur sequentially, and levels of Ypt31/32 peak during cargo sorting. Disrupting either Ypt31/32 function or decreasing Golgi Arf levels lowers the fidelity of cargo sorting, but to different extents. Our findings indicate that Ypt31/32 stimulation of Sec7 activity is a critical driver of cargo sorting at the TGN, providing an explanation for the role of Ypt31/32 and Rab11 family members in vesicle biogenesis. Given the roles of Arl1 and Ypt1 in vesicle tethering, we propose that Sec7 serves as a master regulator to balance incoming and outgoing traffic at the Golgi.

Results

Sec7 localization and activity is regulated by several conserved C-terminal HDS (Homology Downstream of Sec7) domains. The HDS1 domain exerts an autoinhibitory effect that is relieved by binding to Arf1-GTP on the membrane surface. The HDS2-4 domains are also autoinhibitory, but it is unknown how this autoinhibition is relieved (Richardson et al., 2012). An unknown protein might bind to this region to relieve autoinhibition; therefore, we performed a targeted screen of candidate Golgi-localized proteins, testing for factors that either affected Sec7 membrane localization *in vivo* or could recruit Sec7 to membranes *in vitro*.

Sec7 is an effector of the Ypt1 and Ypt31/32 Rab GTPases

Both Rab and Arf GTPases are active at membrane surfaces. Using purified membrane-anchored GTPases to mimic the physiological context of Rab and Arf function, we found that both Ypt1 and Ypt31 Rab proteins recruited a purified Sec7 construct, Sec7_f (encoding residues 203-2009, the essential primary sequence (Richardson et al., 2012)), to liposomes in a nucleotide-dependent manner (Figures 1A and S1A-D). Arl1 also recruited Sec7_f to liposomes (Figure 1B), confirming the conservation of the interaction between Arl1 and BIG1/2 (Christis and Munro, 2012). Another Golgi-localized Rab, Ypt6, did not recruit Sec7_f to liposomes. This result, together with the observed nucleotide-dependence, establishes the specificity of the interactions (Figure 1B).

We imaged Sec7 in mutant strains (Figure S1E) to assess the importance of these interactions for localization to the TGN. Sec7-GFP was largely mislocalized to the cytoplasm in a *ypt1-3* temperature sensitive (ts) strain at the restrictive temperature (Figures 1C and S1F); however, this mutation has many effects on the Golgi, so it is possible that this

effect is indirect. Sec7-GFP exhibited normal localization in *ypt31-101 ypt32* cells at the restrictive temperature (Figures 1C and S1F), indicating that the Ypt31/32 interaction is not required for Sec7 localization to the TGN membrane.

A previous study found allele-specific genetic interactions between Sec7 and both Ypt1 and Ypt31/32: overexpression of Ypt1 suppressed the ts-growth phenotype of the *sec7-1* mutant, and overexpression of Ypt31 or Ypt32 suppressed the ts-growth phenotype of the *sec7-4* mutant (Jones et al., 1999). We confirmed these results and also tested whether overexpression of the other Sec7-interacting proteins, Arf1 and Arl1, was able to suppress the growth phenotypes. Arf1 overexpression partially suppressed the *sec7-1* but not the *sec7-4* mutant (Figure 1D,E); interpretation of this result is complicated because Arf1-GTP is both a regulator and product of Sec7. The *sec7-4* mutant encodes a G883D substitution within the catalytic GEF domain (Deitz et al., 2000), and the isolated GEF domain harboring this mutation exhibits reduced catalytic activity (Jones et al., 1999). We sequenced the *sec7-1* mutant and determined that it encodes a single S402L amino acid substitution in the DCB (Dimerization and Cyclophilin Binding) domain (Figure 1F).

At the restrictive temperature, we observed that GFP-*sec7-4* localized to punctate structures similar to the TGN localization of wild-type GFP-Sec7. In contrast, GFP-*sec7-1* was mislocalized to the cytoplasm under the same conditions (Figures 2A and S1G).

Remarkably, overexpression of Ypt1 suppressed the mislocalization phenotype of GFP-*sec7-1*, restoring the punctate appearance (Figure 2B). The primary established role of Ypt1 is to regulate the tethering of ER-derived vesicles with the *cis*-Golgi (Bacon et al., 1989; Segev, 1991; Cao et al., 1998; Wang et al., 2000). However, Ypt1 alleles that specifically affect fusion of endosomal vesicles with the late Golgi have been described (Sclafani et al., 2010), providing evidence that Ypt1 acts at both early and late Golgi compartments. Our results suggest that Ypt1 also plays a role in Sec7 localization to the TGN through a direct physical interaction.

Mutations in the *SEC7* or *YPT31/32* genes result in similar enlarged Golgi morphology phenotypes (Novick et al., 1980; Benli et al., 1996; Jedd et al., 1997). Given the suppression of the *sec7-4* growth defect by Ypt31/32 overexpression, we tested whether Ypt31/32 could alleviate the catalytic deficiency of the *sec7-4* mutant. We introduced the *sec7-4* mutation into the purified Sec7_f construct (Figure S1B). Using an *in vitro* GEF activity assay measuring the kinetics of Arf1 activation, we observed that the *sec7-4_f* mutant protein exhibits considerably reduced catalytic activity relative to the wild-type protein at the permissive temperature (30°C) (Figure 2C,D). Arf1 activation by *sec7-4_f* displayed sigmoidal kinetics (Figure 2C), indicative of a positive feedback effect under these conditions. Strikingly, the presence of activated Ypt31 in the reaction increased the activity of *sec7-4_f* to a level exceeding that of the wild-type Sec7_f construct (Figure 2D). Ypt31 also exerted a strong stimulatory effect on the activity of the wild-type Sec7_f protein (Figures 2D and 3A). These data indicate that overexpression of Ypt31/32 suppressed the *sec7-4* growth defect by rescuing its catalytic activity. Taken together, our results demonstrate that Sec7 is an effector of both Ypt1 and Ypt31/32 and that these interactions are physiologically relevant.

The four GTPase regulators exert different effects on Sec7 activity

To gain mechanistic insight into the regulation of Sec7, we compared the activity of Sec7_f in the presence of each regulator. Ypt31 and Ypt32 exerted a strong stimulatory effect on Sec7_f, and Ypt1 also stimulated Sec7_f to a significant degree (Figures 3A and S2A-D). Ypt6 had no effect on Sec7_f activity (Figure S2B). Stimulation by Arf1 is most evident at higher concentrations of Arf1 or when the autoinhibitory HDS2-4 domains are removed (Figure 3B and (Richardson et al., 2012)). The stimulatory effect of Ypt31 was dependent upon nucleotide activation *and was* reduced by introduction of the *ypt31-101* mutation (Figure 3C,D). These results establish Ypt31/32 as a potent regulator of Sec7 catalytic activity.

Removing the membrane anchor from Ypt31 eliminated its stimulatory activity (Figure 3D). This result indicates that either proximity of the Rab to the membrane is important for this effect or that the Sec7-Ypt31 interaction is diminished if Ypt31 is not membrane anchored.

Ypt1 and Ypt31 both require the HDS2-3 domains for binding to Sec7_f, suggesting that they bind directly to this region (Figure 3E,F). The effects of Ypt1 and Ypt31 combine to generate an additive stimulatory effect (Figure S2E), implying that Ypt1 and Ypt31 bind simultaneously to different sites within the HDS2-3 domains.

Removal of the HDS4 domain resulted in a Sec7 construct (Sec7⁻HDS4) with activity similar to that of a construct lacking the HDS2-4 domains (Sec7⁻C+HDS1) (Figure 3B,G), indicating that the HDS4 domain is the primary determinant for autoinhibition within the HDS2-4 domains.

Arf1, Arl1, and Ypt31 stimulated the activity of Sec7⁻HDS4, whereas Ypt1 did not (Figure 3G). This indicates that the stimulatory effect of Ypt1 is not observable once autoinhibition *by the HDS4 domain* is relieved, whereas stimulation by Arf1 or Arl1 is more significant in the absence of HDS4 domain autoinhibition. Arf1 and Arl1 stimulated the activity of Sec7⁻C+HDS1 (Figure 3B), whereas Ypt31 exerted no effect, consistent with the lack of Ypt31 binding to this construct (Figure 3E).

In light of the *in vivo* localization data reported here and previously published (Richardson et al., 2012), the *in vitro* GEF assay results (summarized in Figure S2C) signify that Arf1 and Ypt1 mediate recruitment of Sec7 to the TGN and partially relieve autoinhibition (of the HDS1 and HDS4 domains, respectively). Arl1 was weaker than Arf1 in relieving HDS1 domain autoinhibition (Figure 3B,G), and did not increase the activity of Ypt1-stimulated Sec7_f (Figure S2F). These results are consistent with a role for Arl1 in recruitment of Sec7 to the membrane surface, which appears weaker than the roles of both Arf1 and Ypt1. Given its function in localization of the Sec7 homologs BIG1/2 (Christis and Munro, 2012), Arl1 may provide TGN compartment specificity for Sec7 through coincidence with Arf1 and Ypt1.

Ypt31 likely exerts an allosteric effect, perhaps inducing Sec7 to adopt a hyperactive conformation. To test this hypothesis, we measured the activity of Sec7_f anchored to the membrane via a histidine tag. Membrane anchoring almost doubled the activity of the Sec7_f construct (Figure S2G). Ypt1 and Ypt31 each provided further stimulation of the activity of

membrane-anchored Sec7_f (Figure 3H), consistent with both Ypt1 and Ypt31 inducing more active conformations of Sec7. Taken together, these results allow us to construct a model for how the four GTPases recruit Sec7 to the TGN and regulate its activity: Sec7 is initially recruited to the TGN membrane by Ypt1, Arf1, and Arl1 in coincidence, resulting in a basal level of Sec7 activity. Subsequent binding to Ypt31/32 stimulates Sec7 activity (Figure 3I).

Ypt31/32 levels peak during Sec7-dependent cargo sorting events

Our data indicate that Ypt31 is the key regulator of Sec7 GEF activity for Arf1 activation at the TGN. If true, then the appearance of Ypt31 at the TGN should be coincident with Arf1-dependent cargo sorting events. We therefore used live-cell imaging to establish the dynamics of Sec7 at the TGN relative to its regulators and relative to cargos whose sorting depends upon Sec7 activity. As others have reported (Jian et al., 2010), we found that tagging Arf1 or Arl1 inactivated these proteins, so we limited our analysis of regulators to Ypt1 and Ypt31.

The yeast Golgi is very dynamic, with a lifetime of a few minutes (Losev et al., 2006; Matsuura-Tokita et al., 2006; Rivera-Molina and Novick, 2009). Two waves of cargo adaptors are recruited to the TGN, separated by only a few seconds (Daboussi et al., 2012). Our time-lapse imaging revealed that ~500 nm TGN compartments, labeled by Sec7, disintegrate into several smaller structures (Figure 4A-C, Movie S1). These structures appear to be membranous, as they co-label with the integral membrane v-SNARE protein Snc1 (Figure 4D), which marks secretory vesicles destined for the PM. We interpret these small, highly mobile structures to be nascent vesicles or vesicle precursors.

In support of the role of Ypt1 in Sec7 recruitment, we observed that Ypt1 levels peak before Sec7 levels, whereas Ypt31/32 levels peak soon after Sec7 levels (Figures 4E,F, S3A,D, Movie S2, and (Suda et al., 2013)). We examined three cargos: Kex2, a furin protease that cycles between the TGN and endosomes; Tlg1, a Golgi t-SNARE that also cycles between the TGN and endosomes, and Snc1. Kex2 (and presumably Tlg1) is sorted by the Arf1-dependent GGA and AP-1 clathrin adaptors (Abazeed and Fuller, 2008); the sorting machinery for Snc1 is unknown. For each cargo, we measured the time between its disappearance from a Golgi compartment (interpreted as sorting) and the ultimate disintegration of the same compartment. We observed a pattern in which Kex2 was sorted first, followed by Tlg1, then Snc1 (Figures 4E,G, and S3B, Movie S3). Sorting of all three cargos occurred within 15 seconds, consistent with the timing reported for clathrin adaptor progression (Daboussi et al., 2012). Thus, Sec7-dependent cargo sorting events appear to occur sequentially, as previously proposed (Daboussi et al., 2012), with the bulk of sorting to endosomes occurring before sorting to the PM.

Our analysis indicates that Kex2 and Tlg1 sorting occurs soon after Sec7 levels peak, when Ypt31 levels are rising. Disruption of Ypt31/32 function alters the steady-state distribution of Kex2 and Snc1 (Chen et al., 2005). Similarly, we found that lowering Golgi Arf levels by ~90% alters the steady state localization of Kex2 and the kinetics of Tlg1 cargo sorting (Figure S4A-D). Our results lead to a model in which abundant Arf1-GTP, generated by Ypt31/32 stimulation of Sec7 and enhanced by positive feedback, is required for the fidelity of sequential cargo sorting events (Figure 4H). Vesicles formed later in the sequence would

carry more Ypt31/32, enriching these Rab proteins specifically on secretory vesicles. An attractive feature of this model is that after vesicle biogenesis, Sec7 dissociation from a secretory vesicle would allow Ypt31/32 to recruit its known effectors Sec2 and Myo2 (Ortiz et al., 2002; Lipatova et al., 2008; Daboussi et al., 2012), priming the vesicle for motor-driven transport and eventual fusion with the PM.

Discussion

Crosstalk has previously been demonstrated between Arf and Rab pathways during endocytosis (Chesneau et al., 2012), on endosomes (Inoue et al., 2008; Kobayashi and Fukuda, 2012; D'Souza et al., 2014), and at the early Golgi (Chen et al., 2011). Our findings reveal an unprecedented level of crosstalk between Arf and Rab GTPase pathways at the TGN and establish Sec7 as a GTPase signaling hub.

Previous studies identified a role for Ypt31/32 and Rab11 in vesicle formation (Benli et al., 1996; Ullrich et al., 1996; Jedd et al., 1997). Our results provide a mechanistic explanation for Ypt31/32 function in vesicle biogenesis through direct stimulation of Sec7 activity. Cells therefore use a single regulator (Ypt31/32) to drive two coupled events at the TGN: vesicle formation and motor-dependent transport of secretory vesicles. Given the high degree of homology between Ypt31/32 and Rab11-family members (including Rab4 and Rab14), and between Sec7 and the BIG1/2 Arf-GEFs in other organisms, we expect that a similar mechanism operates to generate vesicles at the TGN and recycling endosomes in metazoan cells.

We have also identified Ypt1 as a key regulator of Sec7 membrane localization and activity, underscoring the importance of Ypt1 and Rab1 in regulating multiple aspects of Golgi function. As other known effectors of both Ypt1 and Arl1 mediate tethering of incoming vesicles at the Golgi (Cao et al., 1998; Panic et al., 2003; Setty et al., 2003), direct regulation by these GTPases suggests that Sec7 provides a mechanistic link between incoming and outgoing vesicle traffic (Figure S4E,F).

We found that the *sec7-1* allele encodes a mutation that results in cytoplasmic mislocalization. It is possible that this mutation disrupts the interaction between Sec7 and one of the regulatory GTPases or between Sec7 and the membrane surface. Ypt1 overexpression likely restores membrane localization of the *sec7-1* protein by strengthening the Ypt1-Sec7 interaction, compensating for whichever interaction is diminished by the *sec7-1* mutation. However, we cannot rule out the possibility that Sec7 function is also regulated indirectly by the effect of Ypt1 on Golgi morphology.

The regulation of Sec7 GEF activity is complex. Both the HDS1 and HDS4 domains exert autoinhibitory effects (this work and (Richardson et al., 2012)). Relief of HDS1 domain autoinhibition appears to require recruitment to the membrane surface by binding to either Arf1-GTP or Arl1-GTP, while relief of HDS4 domain autoinhibition appears to require binding of either Ypt1-GTP or Ypt31/32-GTP. The stimulatory effect of Ypt31/32 is greater than that obtained by removal of the HDS4 domain, implying that Ypt31/32 triggers allosteric activation in addition to relief of autoinhibition. Our previous work demonstrated

that the membrane surface itself plays an important role in stimulating Sec7 activity (Richardson et al., 2012), but so far no specific lipid requirement has been identified. Future studies will be needed to determine the mechanistic details underlying membrane recruitment and progression of Sec7 from inactive to fully active states.

Our data, together with previous reports (Christis and Munro, 2012; Richardson et al., 2012; Lowery et al., 2013), indicate that Arf1, Arl1, and Ypt1 each play a role in recruiting Sec7 to the Golgi. Subsequent binding to Ypt31/32 further stimulates the activity of Sec7, and this appears necessary to faithfully drive Sec7-dependent cargo sorting events. This idea is supported by the loss of cargo-sorting fidelity in both *ypt31/32* and *arf1* mutant cells.

Regulation by multiple GTPases is a mechanism to ensure precise spatiotemporal regulation of Sec7 activity. We envision that the integration of four different GTPase signals by Sec7 may enable regulation of TGN cargo sorting in response to various cellular stimuli, including stresses such as nutrient deprivation or changes in secretory cargo load. A full understanding of the signaling logic of the Golgi complex will require mechanistic investigations of each of the Arf and Rab GEFs that together control the function of this organelle.

Experimental Procedures

Plasmid constructs, yeast strains and genetic methods

Plasmids and strains were constructed using standard techniques and are described in Supplemental Experimental Procedures.

Protein purification

Sec7_f and Sec7_C+HDS1 constructs were purified as previously described (Richardson et al., 2012), with the addition of treatment by TEV-protease to remove the 6xHis-tag prior to the final chromatography step. The *sec7-4_f* and Sec7_{HDS4} constructs were purified using the same procedure as Sec7_f. We were not able to purify a well-behaved construct for the HDS2-3 domain region. In our experience, the N-terminal domains of Sec7 appear to be required for the expression and purification of truncation constructs.

C-terminal 7xHis-tagged yeast Rab constructs were created using the pGEX-6P vector backbone and designed so that the C-terminal cysteine residues (prenylated *in vivo*) were replaced with a 7xHis-tag for membrane anchoring. These constructs were purified using the GST tag, which was removed by PreScission protease treatment. Further purification details are included in Supplemental Experimental Procedures. We note that there are two distinct species in some of the Rab purifications. Analysis by anti-His-tag immunoblot indicated that the faster migrating species are likely N-terminal proteolytic products (Figure S1C). Myristoylated-Arf1 was purified as reported (Ha et al., 2005). For purification of myristoylated-Arl1, a plasmid encoding full-length yeast Arl1 was introduced into BL21(DE3) *E. coli* cells together with the Nmt1 plasmid encoding the N-myristoyl transferase enzyme. Growth and expression was the same as for Arf1. Further purification details are included in Supplemental Experimental Procedures. We note that the purified Arl1 protein runs as three species on an SDS-PAGE gel.

Liposome preparation

TGN-like liposomes were prepared as described (Richardson et al., 2012), except they also contained 5% Ni²⁺-DOGS for binding His-tagged proteins. Liposomes were extruded through 100 nm filters.

Liposome flotation (binding) assays

Flotation assays were performed as described (Richardson et al., 2012), using 4 ug of each protein and 0.3 mM of liposomes per 75 ul binding reaction.

GEF activity assays

Tryptophan fluorescence GEF assays were performed at 30°C as described (Richardson et al., 2012). Figure S2A presents an example of a single replicate.

Microscopy

See Supplemental Experimental Procedures for which strains and plasmids were used for each experiment. Images in the same figure panel are shown at the same light levels.

Cells were grown in synthetic media and imaged in log phase (OD₆₀₀ ~ 0.4) on glass coverslips or in glass-bottomed dishes. Images shown in Figures 1,2, and S1 were obtained using a DeltaVision RT wide-field microscope (Applied Precision). Single focal planes are shown after deconvolution in softWoRx.

Images shown in Figures 4, S4, and all Supplemental Movies were obtained using an Andor Revolution spinning disk confocal microscope with dual cameras for simultaneous red/green image acquisition. A single focal plane was imaged under reduced laser power to minimize photobleaching. 500 ms exposures were acquired every second for four minutes at 26°C. Image processing for these data was done using SlideBook software (3I).

Peak-to-peak times were determined similar to a previous report (Daboussi et al., 2012), being careful to only analyze compartments that remained spatially resolved from other compartments and within the observed focal plane for the duration of the analysis time. Peak times were determined after photobleach correction and normalization of the fluorescence signal. The typical amount of photobleaching during a 4 minute time course was ~15% for Sec7-6xDsRed, and ~40-50% for the GFP-tagged proteins. Relative disappearance times were determined using compartments which met the above criteria and for which the disintegration of the Sec7 marker was observable during the observation period. For compartments meeting this criteria, the time of disappearance was chosen as the timepoint when the normalized fluorescence signal dropped below 20% of its maximum value for the duration of the analysis time. We note that although we were only able to quantify several compartments due to the selection criteria, we observed that virtually all compartments exhibited qualitatively similar maturation kinetics.

We tested two different GFP-Ypt31 constructs, one with an expression level much lower than endogenous Ypt31, and another with an expression level that was higher (Figure S3C). Both constructs exhibited similar dynamics relative to Sec7 (Figure S3D), despite differing

in expression level by an order of magnitude. The data shown in Figure 4 was collected using the strain with higher GFP-Ypt31 expression level. Both the GFP-Ypt1 and GFP-Ypt31 fusions were previously shown to be functional (Buvelot Frei et al., 2006).

We were concerned that the measured disappearance times might simply be an artifact of either photobleaching or the intensity of the fluorescence signal (i.e., cargos with weak fluorescent signal may appear to be sorted earlier). Photobleaching was judged not to be a concern based on the total amount of photobleaching (as described above), and considering that other compartments within the same cell remained fluorescent after the disappearance of signal from the measured compartment. To test the possibility of artifacts due to fluorescence intensity, we plotted relative disappearance time versus maximum fluorescence intensity values, averaged for each cargo or mutant strain. There was no significant correlation between compartment fluorescence intensity and disappearance time (Figure S3F), although *Snc1* was the most intense and had the latest disappearance. For example, the intensity of GFP-Tlg1 at Golgi compartments is increased in the *arf1* strain relative to wild-type cells, likely owing to the enlargement of the Golgi in this strain, yet the disappearance of GFP-Tlg1 occurs earlier in this strain relative to the wild-type strain.

Statistical tests

For Figures 2, 3, 4G, and S2D-F, significance was determined by one-way ANOVA with Tukey's test for multiple comparison. For the data in Figure 3A,D,H the variances were not equal among the samples, presumably due to the much faster rates in the Ypt31-stimulated reactions. Therefore, these data were \log_{10} transformed for statistical analysis to equalize the variances prior to performing the ANOVA/Tukey's test. For Figures 4F and S4D, significance was determined by an unpaired T-test with Welch's correction.

Supplementary Material

Refer to Web version on PubMed Central for supplementary material.

Acknowledgments

The authors thank the labs of N. Segev, B. Glick, T. Graham, R. Collins, H. Pelham, and C. Barlowe for reagents. We thank B. Richardson for technical advice, discussions, and reading of the manuscript. We thank S. Emr and T. Bretscher for discussions, use of equipment, gifts of reagents, and reading of the manuscript. This work was funded by NIH grant R01GM098621, and by NIH training grant T32GM007273 to C.M.

References

- Abazeed ME, Fuller RS. Yeast Golgi-localized, gamma-Ear-containing, ADP-ribosylation factor-binding proteins are but adaptor protein-1 is not required for cell-free transport of membrane proteins from the trans-Golgi network to the prevacuolar compartment. *Mol. Biol. Cell.* 2008; 19:4826–4236. [PubMed: 18784256]
- Bacon RA, Salminen A, Ruohola H, Novick P, Ferro-Novick S. The GTP-binding protein Ypt1 is required for transport in vitro: the Golgi apparatus is defective in ypt1 mutants. *J. Cell Biol.* 1989; 109:1015–1022. [PubMed: 2504726]
- Barr FA. Rab GTPase function in Golgi trafficking. *Semin Cell Dev Biol.* 2009; 20:780–783. [PubMed: 19508857]

- Benli M, Doring F, Robinson DG, Yang X, Gallwitz D. Two GTPase isoforms, Ypt31p and Ypt32p, are essential for Golgi function in yeast. *EMBO J.* 1996; 15:6460–6475. [PubMed: 8978673]
- Buvelot Frei S, Rahl PB, Nussbaum M, Briggs BJ, Calero M, Janeczko S, Regan AD, Chen CZ, Barral Y, Whittaker GR, et al. Bioinformatic and comparative localization of Rab proteins reveals functional insights into the uncharacterized GTPases Ypt10p and Ypt11p. *Mol. Cell Biol.* 2006; 26:7299–7317. [PubMed: 16980630]
- Cao X, Ballew N, Barlowe C. Initial docking of ER-derived vesicles requires Uso1p and Ypt1p but is independent of SNARE proteins. *EMBO J.* 1998; 17:2156–2165. [PubMed: 9545229]
- Casanova JE. Regulation of Arf activation: the Sec7 family of guanine nucleotide exchange factors. *Traffic.* 2007; 8:1476–1485. [PubMed: 17850229]
- Chen S, Cai H, Park SK, Menon S, Jackson CL, Ferro-Novick S. Trs65p, a subunit of the Ypt1p GEF TRAPP II, interacts with the Arf1p exchange factor Gea2p to facilitate COPI-mediated vesicle traffic. *Mol. Biol. Cell.* 2011; 22:3634–3644. [PubMed: 21813735]
- Chen SH, Chen S, Tokarev AA, Liu F, Jedd G, Segev N. Ypt31/32 GTPases and their novel F-box effector protein Rcy1 regulate protein recycling. *Mol. Biol. Cell.* 2005; 16:178–192. [PubMed: 15537705]
- Chesneau L, Dambournet D, Machicoane M, Kouranti I, Fukuda M, Goud B, Echard A. An ARF6/Rab35 GTPase cascade for endocytic recycling and successful cytokinesis. *Curr. Biol.* 2012; 22:147–153. [PubMed: 22226746]
- Christis C, Munro S. The small G protein Arl1 directs the trans-Golgi-specific targeting of the Arf1 exchange factors BIG1 and BIG2. *J. Cell Biol.* 2012; 196:327–335. [PubMed: 22291037]
- D'Souza RS, Semus R, Billings EA, Meyer CB, Conger K, Casanova JE. Rab4 Orchestrates a Small GTPase Cascade for Recruitment of Adaptor Proteins to Early Endosomes. *Curr. Biol.* 2014
- Daboussi L, Costaguta G, Payne GS. Phosphoinositide-mediated clathrin adaptor progression at the trans-Golgi network. *Nat. Cell Biol.* 2012; 14:239–248. [PubMed: 22344030]
- Deitz SB, Rambourg A, Kepes F, Franzusoff A. Sec7p directs the transitions required for yeast Golgi biogenesis. *Traffic.* 2000; 1:172–183. [PubMed: 11208097]
- Donaldson JG, Jackson CL. ARF family G proteins and their regulators: roles in membrane transport, development and disease. *Nat. Rev. Mol. Cell Biol.* 2011; 12:362–375. [PubMed: 21587297]
- Ha VL, Thomas GM, Stauffer S, Randazzo PA. Preparation of myristoylated Arf1 and Arf6. *Methods Enzymol.* 2005; 404:164–174. [PubMed: 16413267]
- Inoue H, Ha VL, Prekeris R, Randazzo PA. Arf GTPase-activating protein ASAP1 interacts with Rab11 effector FIP3 and regulates pericentrosomal localization of transferrin receptor-positive recycling endosome. *Mol. Biol. Cell.* 2008; 19:4224–4237. [PubMed: 18685082]
- Jedd G, Mulholland J, Segev N. Two new Ypt GTPases are required for exit from the yeast trans-Golgi compartment. *J. Cell Biol.* 1997; 137:563–580. [PubMed: 9151665]
- Jian X, Cavenagh M, Gruschus JM, Randazzo PA, Kahn RA. Modifications to the C-terminus of Arf1 alter cell functions and protein interactions. *Traffic.* 2010; 11:732–742. [PubMed: 20214751]
- Jones S, Jedd G, Kahn RA, Franzusoff A, Bartolini F, Segev N. Genetic interactions in yeast between Ypt GTPases and Arf guanine nucleotide exchangers. *Genetics.* 1999; 152:1543–1556. [PubMed: 10430582]
- Kobayashi H, Fukuda M. Rab35 regulates Arf6 activity through centaurin-beta2 (ACAP2) during neurite outgrowth. *J. Cell Sci.* 2012; 125:2235–2243. [PubMed: 22344257]
- Lipatova Z, Tokarev AA, Jin Y, Mulholland J, Weisman LS, Segev N. Direct interaction between a myosin V motor and the Rab GTPases Ypt31/32 is required for polarized secretion. *Mol. Biol. Cell.* 2008; 19:4177–4187. [PubMed: 18653471]
- Losev E, Reinke CA, Jellen J, Strongin DE, Bevis BJ, Glick BS. Golgi maturation visualized in living yeast. *Nature.* 2006; 441:1002–1006. [PubMed: 16699524]
- Lowery J, Szul T, Styers M, Holloway Z, Oorschot V, Klumperman J, Sztul E. The Sec7 guanine nucleotide exchange factor GBF1 regulates membrane recruitment of BIG1 and BIG2 guanine nucleotide exchange factors to the trans-Golgi network (TGN). *J. Biol. Chem.* 2013; 288:11532–11545. [PubMed: 23386609]
- Matsuura-Tokita K, Takeuchi M, Ichihara A, Mikuriya K, Nakano A. Live imaging of yeast Golgi cisternal maturation. *Nature.* 2006; 441:1007–1010. [PubMed: 16699523]

- Miserey-Lenkei S, Chalancon G, Bardin S, Formstecher E, Goud B, Echard A. Rab and actomyosin-dependent fission of transport vesicles at the Golgi complex. *Nat. Cell Biol.* 2010; 12:645–654. [PubMed: 20562865]
- Mizuno-Yamasaki E, Rivera-Molina F, Novick P. GTPase networks in membrane traffic. *Annu. Rev. Biochem.* 2012; 81:637–659. [PubMed: 22463690]
- Novick P, Field C, Schekman R. Identification of 23 complementation groups required for post-translational events in the yeast secretory pathway. *Cell.* 1980; 21:205–215. [PubMed: 6996832]
- Ortiz D, Medkova M, Walch-Solimena C, Novick P. Ypt32 recruits the Sec4p guanine nucleotide exchange factor, Sec2p, to secretory vesicles; evidence for a Rab cascade in yeast. *J. Cell Biol.* 2002; 157:1005–1015. [PubMed: 12045183]
- Panic B, Whyte JR, Munro S. The ARF-like GTPases Arl1p and Arl3p act in a pathway that interacts with vesicle-tethering factors at the Golgi apparatus. *Curr. Biol.* 2003; 13:405–410. [PubMed: 12620189]
- Richardson BC, McDonold CM, Fromme JC. The Sec7 Arf-GEF is recruited to the trans-Golgi network by positive feedback. *Dev. Cell.* 2012; 22:799–810.
- Rivera-Molina FE, Novick PJ. A Rab GAP cascade defines the boundary between two Rab GTPases on the secretory pathway. *Proc. Natl. Acad. Sci. USA.* 2009; 106:14408–14413. [PubMed: 19666511]
- Sclafani A, Chen S, Rivera-Molina F, Reinisch K, Novick P, Ferro-Novick S. Establishing a role for the GTPase Ypt1p at the late Golgi. *Traffic.* 2010; 11:520–532. [PubMed: 20059749]
- Segev N. Mediation of the attachment or fusion step in vesicular transport by the GTP-binding Ypt1 protein. *Science.* 1991; 252:1553–1556. [PubMed: 1904626]
- Setty SR, Shin ME, Yoshino A, Marks MS, Burd CG. Golgi recruitment of GRIP domain proteins by Arf-like GTPase 1 is regulated by Arf-like GTPase 3. *Curr. Biol.* 2003; 13:401–404. [PubMed: 12620188]
- Suda Y, Kurokawa K, Hirata R, Nakano A. Rab GAP cascade regulates dynamics of Ypt6 in the Golgi traffic. *Proc. Natl. Acad. Sci. USA.* 2013; 110:18976–18981. [PubMed: 24194547]
- Ullrich O, Reinsch S, Urbe S, Zerial M, Parton RG. Rab11 regulates recycling through the pericentriolar recycling endosome. *J Cell Biol.* 1996; 135:913–924. [PubMed: 8922376]
- Wang W, Sacher M, Ferro-Novick S. TRAPP stimulates guanine nucleotide exchange on Ypt1p. *J. Cell Biol.* 2000; 151:289–296. [PubMed: 11038176]

Highlights

- Sec7 is an effector of the Ypt1 (Rab1) and Ypt31/32 (Rab11) GTPases
- Ypt1 mediates recruitment of Sec7 to the TGN
- Ypt31/32 dramatically stimulates Sec7 activity
- Ypt31/32 levels peak during Sec7-dependent cargo sorting events

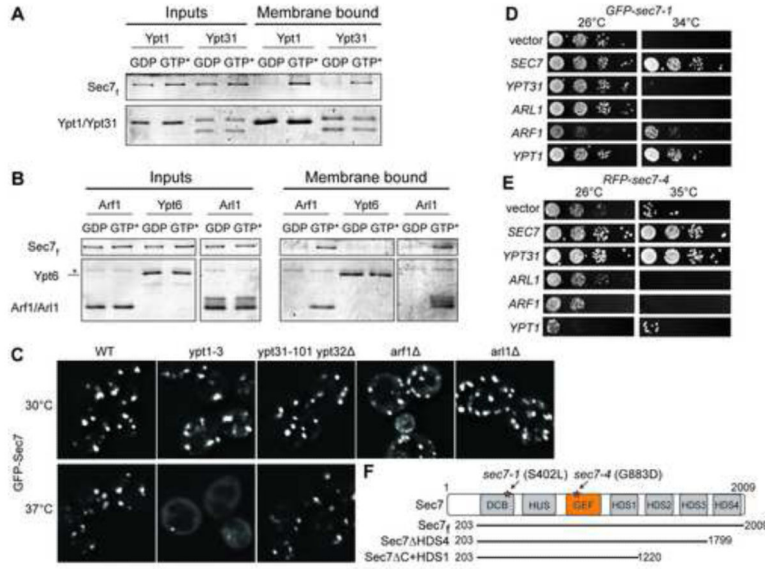


Figure 1. Sec7 is an effector of four different Golgi GTPases

(A) Liposome flotation assays showing activated Ypt1 and Ypt31 recruit purified Sec7_f to liposomes. GTP* = GMP-PNP (active GTPase).

(B) Activated Arf1 and Arl1, but not Ypt6, recruit purified Sec7_f to liposomes. *, contaminant. Purified Rab GTPases bind to membranes regardless of their nucleotide state via a 7xHis tag, which is not present on purified Arf1 or Arl1.

(C) Localization of an extra copy of GFP-Sec7 in yeast cells harboring the indicated mutations. For temperature-sensitive mutants, images are shown for both permissive (30°C) and restrictive (37°C) temperatures.

(D-E) Overexpression of indicated GTPases via 2-μm plasmids in temperature-sensitive yeast cells carrying (D) GFP-sec7-1 or (E) RFP-sec7-4 mutant alleles.

(F) Schematic diagram of the Sec7 conserved domain structure and Sec7 truncated constructs; stars denote the approximate locations of the specified mutations. See also Figure S1.

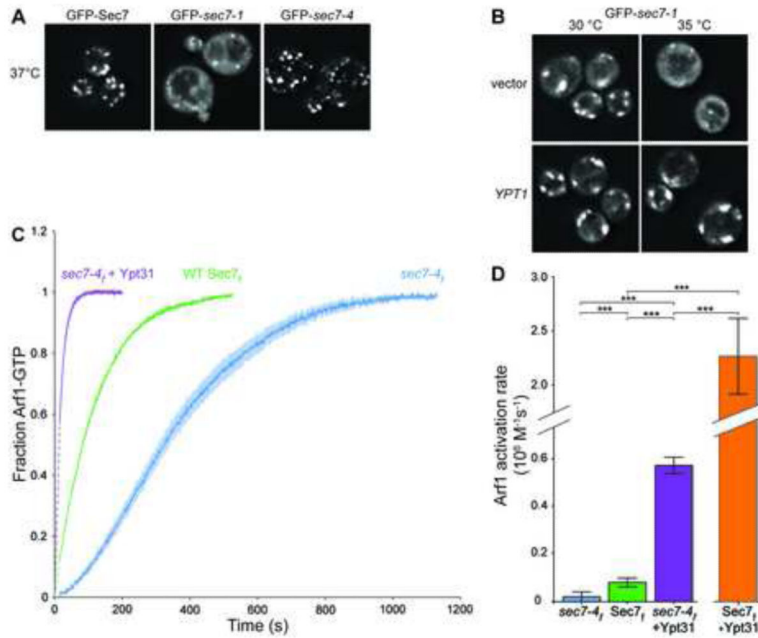


Figure 2. Overexpression of Ypt1 and Ypt31 rescues Sec7 allele-specific phenotypes

(A) Localization of GFP-tagged Sec7, *sec7-1*, and *sec7-4* after 20 min incubation at restrictive temperature (37°C).

(B) Localization of GFP-*sec7-1* in cells overexpressing Ypt1 at both permissive (30°C) and restrictive (35°C) temperatures.

(C) Activation of Arf1 (measured via tryptophan fluorescence) by 100 nM WT Sec7_f, *sec7-4_f*, or *sec7-4_f* in the presence of 500 nM activated Ypt31. Dark lines represent the average of 3 normalized reactions; lighter shaded areas represent the corresponding 95% confidence intervals (CI); dashed lines represent data not captured but inferred from curve-fitting.

(D) Quantification of Arf1 activation rates from curves in (C). Data for WT Sec7_f + Ypt31 is included for comparison. The activation curve for this sample is not shown in (C) because it was acquired using a different concentration (30 nM) of the GEF. Error bars represent 95% CIs for n=3.

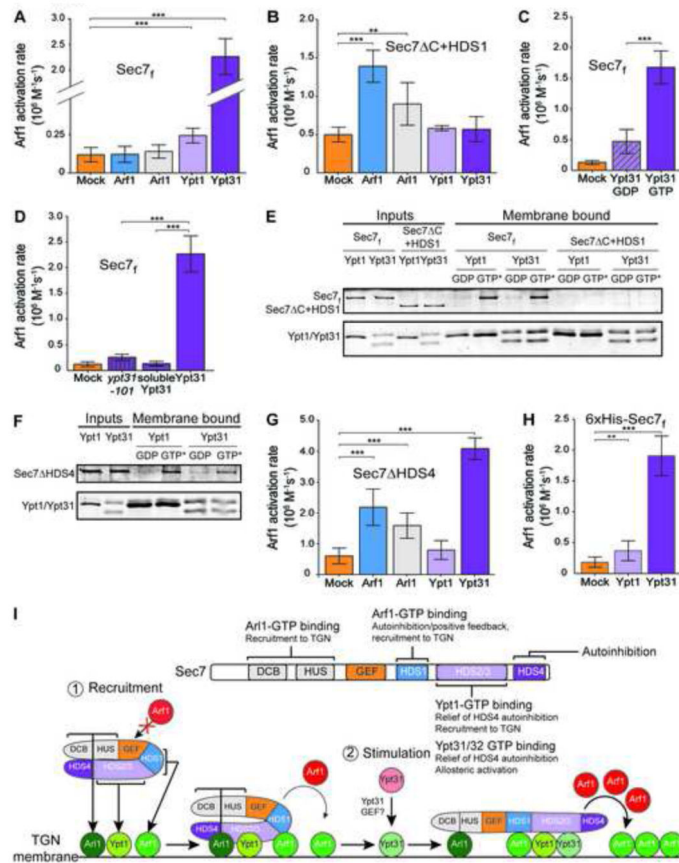


Figure 3. Each GTPase plays a distinct role in Sec7 activation, with Ypt31 exerting the largest stimulatory effect

- (A) Rates of Arf1 activation by Sec7_f in the presence of membrane-bound, activated GTPases or buffer (“mock”). n=3.
- (B) Arf1 activation by purified Sec7_f C+HDS1. n=3.
- (C) Arf1 activation by Sec7_f in the presence of GDP-bound or GTP-bound Ypt31. n=4.
- (D) Arf1 activation by Sec7_f in the presence of activated membrane-bound Ypt31 or *ypt31-101*, or soluble Ypt31. n=3.
- (E,F) Liposome floatation assays showing Ypt1- and Ypt31-dependent recruitment of purified Sec7_f (E) and Sec7 Δ HDS4 (F), but not of purified Sec7_f C+HDS1 (E); GTP* = GMP-PNP (active GTPase).
- (G) Arf1 activation by purified Sec7 Δ HDS4. n=3.
- (H) Arf1 activation by membrane-anchored Sec7_f. n=3.
- (I) Model of Sec7 recruitment to the TGN and regulation of GEF activity by four GTPases. Sec7 is dimeric, but a monomer is shown for simplicity. This model is based on the findings from this study and previous reports (Christis and Munro, 2012; Richardson et al., 2012). See also Figure S2.
- In (A)-(D),(G),(H), error bars represent 95% CIs for the indicated n.

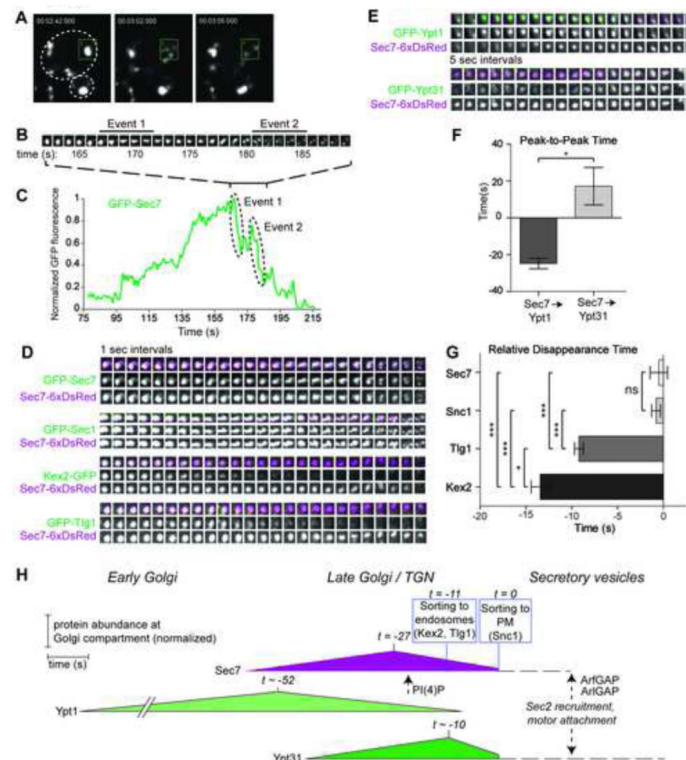


Figure 4. Sec7-dependent cargo sorting events are sequential and coincide with the peak of Ypt31 levels

(A) Live-cell imaging of GFP-Sec7-labeled TGN compartments disintegrating into smaller, fast-moving structures.

(B) Timelapse subseries (1 sec intervals) of the box from (A), a single Golgi compartment.

(C) Normalized quantification of the GFP-Sec7 signal in the box from (A).

(D) Timelapses (5 sec intervals) from strains expressing Sec7-6xDsRed and different Sec7-dependent cargos, aligned by measured Sec7 disappearance time. A strain expressing both GFP-Sec7 and Sec7-6xDsRed serves as a control.

(E) Timelapses (1 sec intervals) from strains expressing Sec7-6xDsRed and GFP-Ypt1 or GFP-Ypt31.

(F) Quantification of the peak-to-peak times. Error bars represent s.e.m. for n=5.

(G) Quantification of the relative disappearance time for cargos. Error bars represent s.e.m. for n=4 to 6.

(H) Model for the dynamics of Sec7-dependent events at the late Golgi. Sec7 disappearance is set to $t=0$. Peak times and sorting times are set relative to $t=0$. Sorting times denote when >80% of the cargo has exited the TGN. For simplicity, a single time (-11 s) is used to denote sorting of Kex2 (-13.5 s) and Tlg1 (-9 s). Times are denoted as approximate (\sim) when derived from two sequential relative comparisons. For example, the timing of Sec7 peak levels was measured relative to Sec7 disappearance (Figure S3E), while the peak levels of the Rab proteins were measured relative to the peak of Sec7 (Panel F). Dotted lines and arrows represent events not measured, but inferred from this study and others, for example, the timing of PI(4)P appearance relative to Sec7 (Ortiz et al., 2002; Daboussi et al., 2012). We envision that Sec7 must leave the membrane surface of a secretory vesicle (perhaps

triggered by inactivation of Arf1 and Arl1 by the Gcs1 ArfGAP) before Ypt31/32 can recruit Sec2, leading to Sec4 activation and recruitment of the Myo2 (Myosin V) motor. See also Figures S3, S4, and Movies S1-S3.